

Membrane Mediated Sorting

Timon Idema,¹ Stefan Semrau,² Cornelis Storm,^{1,3} and Thomas Schmidt²

¹*Instituut-Lorentz for Theoretical Physics, Leiden University, Post Office Box 9506, 2300 RA Leiden, The Netherlands*

²*Physics of Life Processes Leiden Institute of Physics, Leiden University, Post Office Box 9506, 2300 RA Leiden, The Netherlands*

³*Department of Applied Physics and Institute for Complex Molecular Systems, Eindhoven University of Technology, Post Office Box 513, NL-5600 MB Eindhoven, The Netherlands*

(Received 14 April 2009; published 13 May 2010)

Inclusions in biological membranes may interact via deformations they induce on the shape of that very membrane. Such deformations are a purely physical effect, resulting in nonspecific forces between the inclusions. In this Letter we show that this type of interaction can organize membrane domains and hence may play an important biological role. Using a simple analytical model we predict that membrane inclusions sort according to the curvature they impose. We verify this prediction by both numerical simulations and experimental observations of membrane domains in phase separated vesicles.

DOI: 10.1103/PhysRevLett.104.198102

PACS numbers: 87.16.dr, 87.17.Aa, 87.53.Ay

Introduction.—On the mesoscopic scale, cellular organization is governed by some well-known forces: hydrophobic, electrostatic, and van der Waals interactions [1]. These forces are responsible for the structure of the lipid bilayer and highly specific protein-protein interactions. However, due to their short range, they do not provide a mechanism for some important biological functions like the recruitment of proteins to certain regions in the plasma membrane. Recently, attention was drawn to another type of interaction: membrane curvature mediated interactions [2–12]. These interactions are known to be long ranged [2] and non-pairwise additive [6]. In this Letter we demonstrate how membrane mediated interactions give rise to long-range order in a biomimetic system. In the membranes of living cells the breaking of the homogeneity by the formation of patterns and long-range order carries significant biological implications for processes like signaling, chemotaxis, exocytosis, and cell division.

A well-suited system to study membrane mediated interactions is a giant unilamellar vesicle (GUV) composed of cholesterol and two other types of lipid, one with high and one with low melting temperature. For many different compositions such GUVs phase separate into liquid ordered (L_o) and liquid disordered (L_d) domains [13–15]. Typically one finds many domains of one phase on a “background” vesicle of the other phase. A line tension on the boundary between the two phases causes the domains to be circular in shape [16–18]. Moreover, domains sometimes partially “bud out” from the spherical vesicle to reduce the boundary length even further [14].

Recent experiments have shown that partially budded membrane domains repel due to membrane mediated interactions [14,19,20]. From measurements of domain fusion dynamics [19] and the distribution of domain sizes [20] it became evident that membrane mediated interactions require a minimum domain size. If domains are too small their curvature equals that of the surrounding mem-

brane. In that case the line tension between the L_o and L_d phase cannot push the domains out of the background membrane. Consequently, domains do not experience any curvature related interaction [20]. As the domain circumference grows due to repeated fusion events the influence of the line tension eventually becomes bigger than that of the bending rigidity and the domain partially buds out. This leads to a repulsive interaction that increases with domain size. Consequently, domain coalescence slows down significantly after reaching a certain preferred size [19–21]. This preferred size can be found as a maximum in the domain size distribution. Although the domains no longer coalesce, they are by no means static, but rather mobile and reorganize continuously. Because larger domains exert a greater force on their neighbors, the domains will collectively try to find a configuration in which larger domains have a larger effective area around them. We expect that, due to this size-dependent interaction, the domains demix by size to achieve an optimal configuration.

We note that this effect is different from depletion interaction in the sense that the distribution of domain sizes in our system is narrow. Moreover, the interaction we consider here is both long ranged and soft, whereas depletion is an effect seen in systems with hard-core repulsions. Depletion may of course still play a small role, but can be ignored in comparison to the membrane mediated interactions discussed here.

In this Letter we present an analytical model in which we analyze the possible distributions of domains on phase-separated vesicles, and find that they exhibit a striking tendency to sort. We complement this model by performing Monte Carlo simulations using realistic membrane parameters that were experimentally obtained in previous work. Both the model and the simulations show that sorting is an unavoidable consequence of the size-dependent nature of the interactions and the finite area available on a vesicle. In addition, we present experimental results on

lipid vesicles, composed of cholesterol and two other types of lipids, which exhibit phase separation, with L_o domains in a L_d background. We find that these domains indeed sort by size. In particular, we find a correlation between the size of a domain and the size of its neighbors, which is reproduced by our simulations.

Analytical model.—A somewhat oversimplified analysis of the total energy of a fully mixed and a fully demixed system gives us a direct clue as to whether the domains segregate into regions of identical-sized ones or not. Because the bending rigidity of the L_o domains is much higher than that of the L_d background [17], we assume the domains to be rigid inclusions. To first approximation, also conical transmembrane proteins can be described in the same way. As was first shown by Goulian *et al.* [2], there is a repulsive potential between two inclusions in an infinite membrane that drops off as $1/r^4$, with r the distance between the inclusions. Moreover, the interaction strength depends on the imposed contact angle at the edge of an inclusion, and for two inclusions with contact angles α and β we have

$$V \sim \frac{\alpha^2 + \beta^2}{r^4}. \quad (1)$$

Although the interactions are not pairwise additive, the qualitative dependence of V on the contact angles and inclusion distance does not change if more inclusions are added to the system [4,6]. It is therefore possible to use a mean-field description for a finite, closed system with many inclusions, from which the prefactor in Eq. (1) can be determined experimentally [20]. Moreover, we can use effective pairwise interactions for nearest-neighbor domains based on their size, as a function of their distance.

For simplicity we look at a system with only two sizes of domains, which we will call “big” and “small” (see Fig. 2). This choice is motivated by earlier experimental results that show a narrow distribution of domain sizes [20]. In our model the most abundant experimental domain size (with a typical radius of $3.0 \mu\text{m}$) corresponds to the small domains. For the big domains we take a radius of $(3.0 \mu\text{m})\sqrt{2} = 4.3 \mu\text{m}$, which means that their area is twice that of the small domains.

Let us denote the number of domains by N , the number of big domains by $N_b = \gamma N$ and that of small domains by $N_s = N - N_b = (1 - \gamma)N$. Likewise we denote the contact angle of a big domain by α_b , that of a small domain by α_s , and the average contact angle of a domain’s nearest neighbors (in the mean-field approach) by β . If we neglect the small curvature of the background sphere, which has surface area A , we can associate an “effective radius” to each domain corresponding to the patch of area which it dominates (i.e., in which it is the closest domain). In a completely mixed system the effective radius of all domains is equal and given by $R_{\text{eff}} = \sqrt{A/(\pi N)}$. In a fully mixed system each of the domains has 6γ big and $6(1 - \gamma)$

small neighbors, which allows us to calculate the potential of that configuration in the mean-field approach:

$$V_{\text{mixed}} = \frac{6}{16} N_b \frac{\alpha_b^2 + \beta^2}{A^2/(\pi^2 N^2)} + \frac{6}{16} N_s \frac{\alpha_s^2 + \beta^2}{A^2/(\pi^2 N^2)}, \quad (2)$$

where $\beta = \gamma\alpha_b + (1 - \gamma)\alpha_s$. In the fully demixed system, the big domains can take up a larger fraction ϕ of the vesicle surface than they occupy in the fully mixed system. By doing so they can increase the distance between them, reducing the interaction energy. The penalty for this reduction is a denser packing of the small domains, but since their repulsive forces are smaller, the total configuration energy can be smaller than in the mixed system. We consider the regions in which we have big and small domains separately and get two effective radii: $R_{\text{eff}}^b = \sqrt{(\phi A)/(\pi N_b)}$ and $R_{\text{eff}}^s = \sqrt{((1 - \phi)A)/(\pi N_s)}$. For the potential energy we obtain

$$V_{\text{demixed}} = \frac{6}{16} N_b \frac{2\alpha_b^2}{(R_{\text{eff}}^b)^4} + \frac{6}{16} N_s \frac{2\alpha_s^2}{(R_{\text{eff}}^s)^4}, \quad (3)$$

where we have assumed the number of domains is large enough that ignoring the boundary between the two regions is justified. For a fully mixed system we would have $\phi = \gamma$; i.e., the area fraction assigned to the big domains is

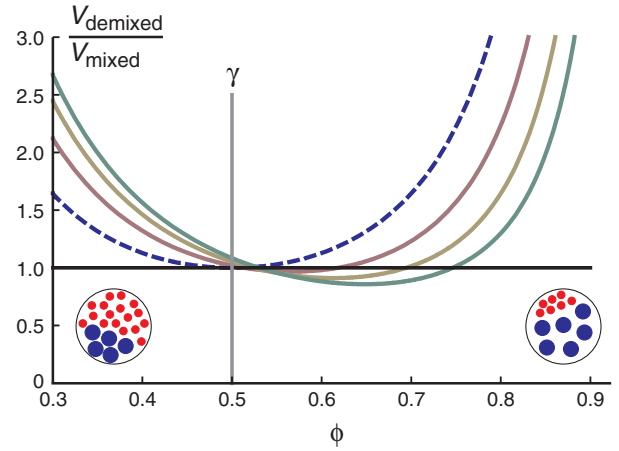


FIG. 1 (color online). Comparison of the potential energies of the completely mixed and completely demixed state of a vesicle with domains of two different sizes. The freely adjustable parameter ϕ denotes the fraction of the vesicle’s surface area claimed by the big domains. The dashed blue (dark gray) line indicates the case in which the “big” and “small” domains are equal in size (and hence have equal contact angles). The solid red, yellow, and green (light gray) lines indicate contact angle ratios α_b/α_s of 1.5, 2.0, and 2.5, respectively. Domain demixing occurs for any value of ϕ for which the potential ratio is less than 1 (black horizontal line). For comparison the number fraction γ of the big domains is indicated by the gray vertical line. Insets: typical distributions of domains for small (left) and big (right) values of ϕ . For small ϕ , the big domains are packed closely together and the small domains claim the largest area fraction, for large ϕ the situation is reversed.

equal to their number fraction. In the demixed system the parameter ϕ becomes freely adjustable and can be tuned to minimize the interaction energy. Comparing the demixed potential Eq. (3) to the mixed potential Eq. (2), we find

$$\frac{V_{\text{demixed}}}{V_{\text{mixed}}} = 2 \left[\frac{\gamma^3}{(1-\gamma)\phi^2} \left(\frac{\alpha_b}{\alpha_s} \right)^2 + \frac{(1-\gamma)^2}{(1-\phi)^2} \right] \times \left[\frac{\gamma(1+\gamma)}{1-\gamma} \left(\frac{\alpha_b}{\alpha_s} \right)^2 + 2\gamma \left(\frac{\alpha_b}{\alpha_s} \right) + (2-\gamma) \right]^{-1}. \quad (4)$$

Plots for several values of the parameters are given in Fig. 1. For a range of values of the adjustable parameter ϕ the energy of the demixed state is smaller than that of the mixed state; this effect becomes more pronounced as the difference in contact angle (and therefore repulsive force) increases. In the configuration which has the lowest total energy the area fraction ϕ claimed by the big domains is indeed larger than their number fraction γ .

Simulations.—In the analytical model we only considered the two extreme configurations of a completely mixed and a completely demixed system. In order to be able to study also intermediate states of the system we performed Monte Carlo simulations. In these simulations we again studied a binary system consisting of small and big do-

main, where the surface area of the big domains is 2 or 3 times larger than that of the small ones. Starting from a random configuration of big and small L_o domains on a L_d sphere, we used Monte Carlo steps to find the energy minimum, and consistently found demixing. A typical example of a relaxation process and a configuration after 5×10^6 time steps are shown in Fig. 2. The potential we used in the simulations is based on Eq. (1) and given by $V = (i^2 + j^2)/r^4$, with i and j the contact angles of the domains, which scale linearly with their radius [20]. Figure 2(o) shows the effect of different number fractions and size ratios between the big and small domains. As predicted by the analytical model, larger size ratios result in larger differences in occupied area. Moreover, we find that demixing occurs faster if the number fractions of the big and small domains are not equal. To verify that the sorting effect we observe is not due to depletion interactions, we also ran simulations with hard-core repulsions. These simulations did not result in any demixing after 10×10^6 time steps.

Complementing the simulations on the binary system, we also ran simulations of a system with an exponential distribution of domain sizes, as found in experiment [20]. In these simulations we also found demixing. Including multiple domain sizes allows for better comparison with

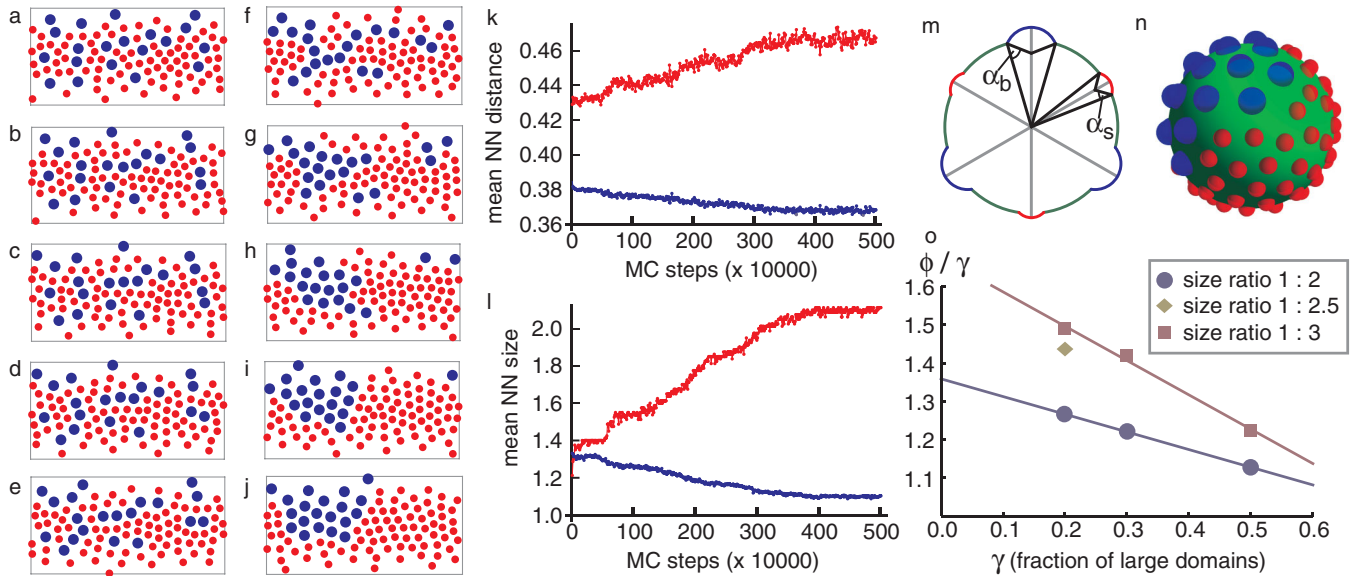


FIG. 2 (color online). Monte Carlo relaxation of a random configuration of 70 small (red, light gray) and 30 big (blue, dark gray) domains on a spherical vesicle. (a)–(j) A folded-open view of the entire vesicle, with the azimuthal angle along the horizontal direction and the polar angle along the vertical direction. The pictures show configurations after (a) 1000 (b) 50 000 (c) 100 000 (d) 200 000 (e) 500 000 and (f) 1, (g) 2, (h) 3, (i) 4, and (j) 5×10^6 steps. (k) Evolution of the mean nearest-neighbor distance over time, split out to large (red, light gray) and small (blue, dark gray) domains. (l) Evolution of the mean nearest-neighbor size over time, split out to large (red, light gray) and small (blue, dark gray) domains. Saturation appears to be reached after approximately 4×10^6 steps. (m) Schematic drawing of a cross section of the vesicle, showing the contact angles α_s and α_b of the small and big domains, respectively. (n) The configuration on a sphere after 5×10^6 time steps. (o) Occupied area fraction of the big domains ϕ as a function of their number fraction γ . The plot shows the effect of different number fractions and domain size ratios on the sorting process. As predicted by the analytical model, larger size ratios result in larger differences in occupied area fractions. Moreover, we find that the speed of demixing increases with decreasing number fraction.

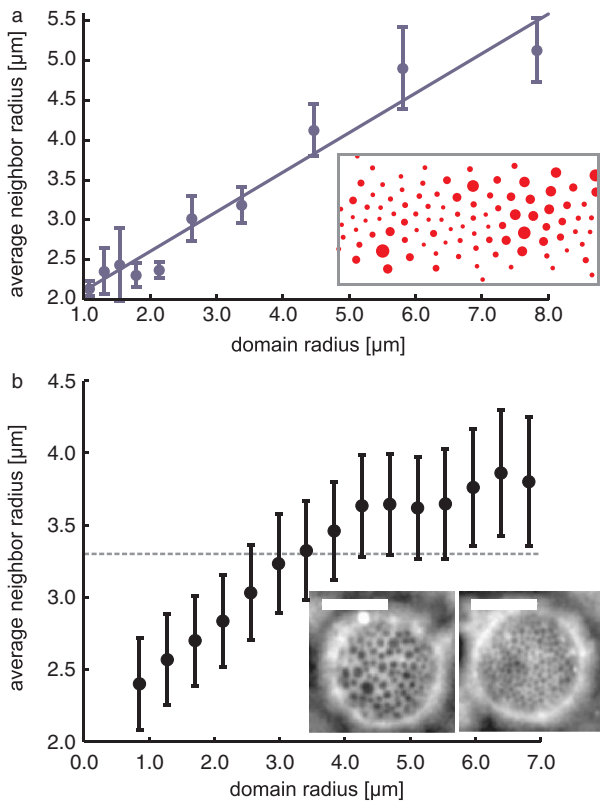


FIG. 3 (color online). Correlations between the size of a domain and that of its nearest neighbors. (a) Correlation plot of a simulation in which the domain sizes follow an exponential distribution. The simulation ran for 15×10^6 steps; error bars obtained using the last 5×10^6 steps. Inset: Example of the actual distribution of domains on the vesicle after 15×10^6 steps. (b) Correlation plot averaged over 21 experimental vesicles; the dashed line corresponds to the average $3.3 \mu\text{m}$. Domain sizes are grouped in equally sized bins. Inset: Two sides of the same vesicle showing very different domain sizes. Scale bar $20 \mu\text{m}$.

experiment; in particular, we can look for correlations between the size of a domain and its nearest neighbors. An example of an obtained correlation plot is shown in Fig. 3(a).

Experimental verification.—Our theoretical prediction that domains segregate into regions of equal-sized ones is confirmed by experimental observations. In experiments detailed in [20], we studied the distribution of budded domains on the entire vesicle. The vesicles we observed were lying on top of other vesicles, preventing distortion due to adhesion to the underlying coverslip. We consistently found that vesicles have regions where some domain sizes are overrepresented. An example of such an experiment is given in the insets of Fig. 3(b), where two sides of the same vesicle are shown. Quantitatively, we found that there is a correlation between the size of a domain and the average size of its nearest neighbors [Fig. 3(b)]. The do-

main sorting occurred consistently in all 21 vesicles with budded domains we studied.

Conclusion.—As we have shown in this Letter, membrane mediated interactions on closed vesicles lead to the sorting of domains by size. Our analysis shows that this is due to the fact that larger domains impose a larger curvature on their surrounding membrane. We expect the same sorting effect to occur for other curvature inducing membrane inclusions, in particular, cone shaped transmembrane proteins. This spontaneous sorting mechanism could potentially be used to create polarized soft particles. Moreover, similar sorting effects may occur in the membranes of living systems without the need of a specific interaction or an actively driven process.

This work was supported by funds from the Netherlands Organization for Scientific Research (NWO-FOM) within the program on Material Properties of Biological Assemblies (FOM-L1707M & FOM-L2601M).

- [1] B. Alberts *et al.*, *Molecular Biology of the Cell* (Garland Science, New York, NY, USA, 2008), 5th ed.
- [2] M. Goulian, R. Bruinsma, and P. Pincus, *Europhys. Lett.* **22**, 145 (1993).
- [3] J.-M. Park and T. C. Lubensky, *J. Phys. I (France)* **6**, 1217 (1996).
- [4] K. S. Kim, J. Neu, and G. Oster, *Biophys. J.* **75**, 2274 (1998).
- [5] T. Chou, K. S. Kim, and G. Oster, *Biophys. J.* **80**, 1075 (2001).
- [6] P. G. Dommersnes and J.-B. Fournier, *Biophys. J.* **83**, 2898 (2002).
- [7] K. Farsad and P. De Camilli, *Curr. Opin. Cell Biol.* **15**, 372 (2003).
- [8] H. T. McMahon and J. L. Gallop, *Nature (London)* **438**, 590 (2005).
- [9] M. M. Müller, M. Deserno, and J. Guven, *Europhys. Lett.* **69**, 482 (2005).
- [10] J. Zimmerberg and M. M. Kozlov, *Nat. Rev. Mol. Cell Biol.* **7**, 9 (2006).
- [11] B. J. Reynwar *et al.*, *Nature (London)* **447**, 461 (2007).
- [12] A. Tian and T. Baumgart, *Biophys. J.* **96**, 2676 (2009).
- [13] C. Dietrich *et al.*, *Biophys. J.* **80**, 1417 (2001).
- [14] T. Baumgart, S. T. Hess, and W. W. Webb, *Nature (London)* **425**, 821 (2003).
- [15] S. L. Veatch and S. L. Keller, *Biochim. Biophys. Acta* **1746**, 172 (2005).
- [16] T. Baumgart, S. Das, W. W. Webb, and J. T. Jenkins, *Biophys. J.* **89**, 1067 (2005).
- [17] S. Semrau *et al.*, *Phys. Rev. Lett.* **100**, 088101 (2008).
- [18] A. R. Honerkamp-Smith *et al.*, *Biophys. J.* **95**, 236 (2008).
- [19] M. Yanagisawa *et al.*, *Biophys. J.* **92**, 115 (2007).
- [20] S. Semrau, T. Idema, T. Schmidt, and C. Storm, *Biophys. J.* **96**, 4906 (2009).
- [21] M. Laradji and P. B. Sunil Kumar, *Phys. Rev. Lett.* **93**, 198105 (2004).